

Cytoskeletal Drugs Modulate Off-Target Protein Folding Landscapes Inside Cells

Caitlin M. Davis^{1,2,†,*} and Martin Gruebele^{1,2,3,*}

¹Department of Chemistry, ²Department of Physics, and ³Center for Biophysics and Quantitative Biology, University of Illinois at Urbana-Champaign, Urbana, IL 61801 USA

KEYWORDS *Crowding Helix Two (CrH2), Cytochalasin D, Cytoskeleton, Fluorescence Resonance Energy Transfer (FRET), Latrunculin B, Nocodazole, Macromolecular Crowding, Phosphoglycerate Kinase (PGK), Protein Folding, Thermal Denaturation, Variable Major Protein-Like Sequence Expressed (VlsE), Vinblastine*

ABSTRACT: The dynamic cytoskeletal network of microtubules and actin filaments can be disassembled by drugs. Cytoskeletal drugs work by perturbing the monomer-polymer equilibrium, thus changing the size and number of macromolecular crowders inside cells. Changes in both crowding and non-specific surface interactions ('sticking') following cytoskeleton disassembly can affect protein stability, structure, and function directly, or indirectly by changing the fluidity of the cytoplasm and altering the crowding and sticking of other macromolecules in the cytoplasm. The effect of cytoskeleton disassembly on protein energy landscapes inside cells has yet to be observed. Here we have measured the effect of several cytoskeletal drugs on the folding energy landscape of two FRET-labeled proteins with different *in vitro* sensitivities to macromolecular crowding: phosphoglycerate kinase (PGK) was previously shown to be more sensitive to crowding, whereas variable major protein-like sequence expressed (VlsE) was previously shown to be more sensitive to sticking. The in-cell effect of drugs that depolymerize either actin filaments (cytochalasin D, latrunculin B) or microtubules (nocodazole, vinblastine) were compared. The crowding sensor protein CrH2-FRET verified that cytoskeletal drugs decrease crowding inside cells despite also reducing overall cell volume. Reduced compactness and folding stability of PGK could be explained by decreased crowding induced by these drugs. VlsE's opposite response to the drugs shows that depolymerization of the cytoskeleton also changes sticking in the cellular milieu. Our results demonstrate that perturbation of the monomer-polymer cytoskeletal equilibrium, for example during natural cell migration or stresses from drug treatment, have off-target effects on the energy landscapes of proteins in the cell.

INTRODUCTION

The energy landscape of proteins is highly dependent on the environment. Proteins have evolved to function under crowded conditions inside cells, where macromolecules exclude as much as 40% of the volume.¹ Macromolecular crowding depends not only on crowder concentration but also on crowder size and shape.² A key example is the cytoskeleton, whose crowder size and shape constantly change through assembly and disassembly of subunits,^{3,4} thereby also affecting the fluidity of the cytoplasm and crowding ability of other macromolecules. Microtubules assemble to form the mitotic spindle during cell division, and their local organization aligns and segregates chromosomes into daughter cells.⁵ Actin dynamics assists with embryonic morphogenesis,^{6,7} immune surveillance,⁸ angiogenesis,⁹ and tissue repair and regeneration.¹⁰ Cell migration requires disassembly of actin filaments at the rear of the cell, which we speculate locally decreases crowding and increases diffusion, assisting cell motility but also changing the local environment of proteins as a side effect.

In addition to excluded volume, proteins in the cell are subject to non-specific 'sticking' to other macromolecular surfaces.^{11–13}

Disassembled cytoskeletal components, such as tubulin dimers, are known to interact strongly with regulatory proteins like stathin,¹⁴ but the exposure of surfaces normally buried in assembled tubules could also lead to sticking to other proteins.

Similarly, monomeric G-actin is present in cells at significant concentration relative to polymeric F-actin.¹⁵

Thus, local assembly or disassembly of the cytoskeleton likely modulates protein stability and compactness broadly, not just proteins associated with cytoskeletal function. Here we measure the effect of cytoskeleton disassembly on the folding reaction of proteins in U-2 OS bone cancer cells treated with drugs that depolymerize actin or tubulin. First, the crowding sensor crowding helix two (CrH2) was used to verify that decreased crowder size decreases macromolecular crowding *in vitro*.¹⁶ The sensor then was transfected transiently into U-2 OS cells, which were evaluated for changes in cell morphology and compaction of the sensor upon incubation with several depolymerizing cytoskeletal drugs. Finally, the stability, compactness, and folding kinetics of two proteins were measured in cells treated with the cytoskeletal drugs: phosphoglycerate kinase (PGK) is more sensitive to crowding, and variable major protein-like sequence expressed (VlsE) is more sensitive to sticking.¹⁷ By measuring changes in protein stability and folding kinetics of both types of proteins in cells with decreased crowder sizes and more exposed crowder surface area, we can quantify how local cytoskeletal rearrangements in the cytoplasm impact protein energy landscapes.

We confirm that cytoskeletal drugs change cell morphology: treated cells are rounded and retracted compared to untreated

cells and have decreased cell volume. Therefore, increased crowding due to decreased cell volume and decreased crowding induced by cytoskeletal disassembly are competing forces inside cells. To determine which force dominates, the CrH2 crowding sensor was expressed in cells treated with the cytoskeletal drugs. We find that the sensor is less compact in treated cells, therefore, changes in crowding associated with cytoskeletal drugs are dominated by smaller crowder size, not by reduced cell volume.

Reduced crowding upon cytoskeletal disassembly can explain changes in the energy landscape of PGK, but not for VlsE. Consistent with decreased crowding as quantified by CrH2, PGK is expanded in size and less stable in treated cells. Disassembly of microtubules resulted in larger differences than disassembly of actin filaments. Two effects contribute to these differences: (1) Microtubules play a larger role in organizing the cytoplasm.^{18,19} (2) Microtubules have a larger monomer-polymer size differential.²⁰ On the other hand, VlsE showed a small but opposite trend: it was slightly compacted and stabilized after disassembly of the cytoskeleton. These observations are consistent with increased sticking of VlsE to disassembled cytoskeletal components. In fact, the sensitivity of VlsE stability and dynamics to its environment are enhanced three-fold in cells compared to *in vitro*.

Our results show that changes to the cytoskeletal network can affect energy landscapes of proteins with very different consequences inside cells via crowding or sticking. Therefore, both natural (cell division, motility) and unnatural (chemotherapy) perturbations of the cytoskeleton impact unrelated cytoplasmic protein interactions such as folding, assembly, and enzymatic reactions.

MATERIALS AND METHODS

Protein Engineering and Expression. CrH2 is a synthetic protein sensor for quantifying macromolecular crowding in bacterial and mammalian cells. It is comprised of two conformationally flexible α -helices in parallel that are compressed when placed in a more crowded environment (Figure 1A).¹⁶ Destabilized variants of PGK and VlsE were selected so that folding could be assessed at temperature ranges where cells are viable. The enzymatically active triple mutant (Y122W/W308F/W333F) of yeast PGK²¹ and bacterial VlsE without the N-terminal lipidation signal²² have melting temperatures of \sim 40 °C.

The plasmids encoding for FRET-labeled crowding helix two (CrH2),¹⁶ yeast phosphoglycerate kinase (PGK),²¹ and *Borrelia burgdorferi* variable major protein-like sequence expressed (VlsE)²² have been described in detail previously. Briefly, the FRET-labeled fusion proteins have AcGFP1 and mCherry at the N and C termini, respectively. A two-amino acid linker connects the protein with each label. Additionally, a Ni affinity His-tag with a thrombin cleavage site was added to the N-terminus of PGK-FRET and CrH2-FRET and the C-terminus of VlsE-FRET for purification of the recombinant protein. The fusion protein sequence was cloned into the pDream 2.1 vector (GenScript Biotech, Piscataway, NJ) which contains a T7 and CMV promoter for dual expression in bacterial and mammalian cells. For temperature calibration, a mCherry construct consisting of an N-terminal His-tag with a thrombin cleavage site and mCherry in the pDream 2.1 vector was generated.

For *in vitro* studies, the proteins were expressed and purified as previously reported.^{17,23} Protein purity was assessed by SDS-PAGE and molecular weight confirmed by low-resolution electrospray ionization mass spectrometry. Circular dichroism and fluorescence spectroscopy confirmed that tertiary structure was not disrupted by labeling or purification. Sample concentrations of 2-3 μ M in 20 mM sodium phosphate buffer at pH 7 were prepared for *in vitro* studies by sandwiching the sample between a coverslip (Fisherbrand, No. 1.5) and microscope slide (Fisherbrand, 1 mm) with a 100 μ m spacer (Grace Bio-Labs, Bend, OR). Identical imaging chambers were used for *in vitro* and in cell studies.

Cell Culture and Transfection. Human bone osteosarcoma epithelial cells (U-2 OS) were cultured and grown to 70% confluence in DMEM (Corning, Corning, NY) + 1% penicillin-streptomycin (Corning) + 10% fetal bovine serum (FBS, ThermoFisher Scientific) media. Transfection was performed with Lipofectamine (Invitrogen) following the manufacturer's protocol. At the time of transfection, cells were split and grown on coverslips. Media was changed six hours after transfection. Cells were imaged 17 hours after transfection.

1000-fold concentrated stock solutions of cytochalasin D (Sigma-Aldrich), latrunculin B (Sigma-Aldrich), nocodazole (Sigma-Aldrich), and vinblastine sulfate salt (Sigma-Aldrich) in DMSO were prepared per the manufacturer's protocol. Final drug concentrations of 1 μ M cytochalasin D,²⁴ 0.1 μ M latrunculin B,²⁴ 0.3 μ M nocodazole,²⁵ and 2.2 μ M vinblastine²⁶ were selected based on previous studies. These cytoskeletal drugs were selected because the response of the U-2 OS cytoskeletal network to them has been well characterized.²⁷⁻²⁹ Ten minutes prior to imaging, cells were placed in imaging chambers filled with optimum (ThermoFisher Scientific) supplemented with 10% FBS and the desired drug.

Fast Relaxation Imaging (FReI). The FReI apparatus has been described previously.²³ Briefly, an infrared laser was used to rapidly perturb the folding equilibrium via heating on a timescale faster than the dynamics of interest. Fluorescence microscopy was then used to probe the folding/unfolding relaxation to equilibrium. A computer-controlled, continuous-wave 2 μ m laser (AdValue Photonics, Tucson, AZ) produced a step-function shaped temperature perturbation. The magnitude of the temperature jump was calculated using the temperature-dependent quantum yield of mCherry excited between 565 and 598 nm.³⁰ The stepped temperature perturbation began at \approx 21 °C and increased to \approx 50 °C in 4 °C steps. The protein was given \approx 9 s (ca. 5 relaxation lifetimes) to relax to its new equilibrium following each jump.

The change in signal induced by the temperature jump was probed in real time by fluorescence microscopy. A white LED (Prizmatix, UHP-T2-LED-White) excited the donor label for FRET excitation by passing the light through an ET470/40x bandpass filter (Chroma, Bellows Falls, VT) and T495lpxt dichroic (Chroma). Alternatively, to excite the acceptor label an ET580/25x bandpass filter (Chroma) and T600lpxr dichroic (Chroma) were used. The excitation was focused onto the sample with a microscopy objective (Zeiss, 63x/0.85 NA N-Achroplan) and the emission was passed through an ET500lp filter (Chroma) and split into two channels (donor/green and acceptor/red) by a T600lpxr dichroic (Chroma) onto a CMOS camera (Lumenera, LT225 NIR/SCI CMOS detector). Images were collected at a frame rate of 25-60 Hz with 16-40 ms integration times. Instrument control and data collection were

controlled using a LabVIEW (National Instruments, Austin, TX) computer program. Data collected with the CMOS detector was converted to a MATLAB (MathWorks, Natick, MA) compatible format and MATLAB was used to separate and align the channels.

Analysis of Thermodynamic Data. Temperature melts of the proteins were collected using the average of the final 4 seconds of the equilibration (flat phase of the step function) after the jump. Thermodynamic data was plotted as the ratio of the donor (D) and acceptor (A) intensities (D/A) vs. temperature. Observed D/A ratios depend on the instrument imaging path (e.g. optics, camera) and cell line (e.g. plasmid expression efficiency) but trends in D/A ratio do not. Therefore, while thermodynamics and kinetics can be quantitatively compared between experiments, absolute D/A ratios are only compared for data collected on the same instrument and cell line, such as in the present study.

The resulting melting curves were fit to an apparent two-state equilibrium model:

$$S(T) = \frac{S_D + m_D(T - T_0) + [S_N + m_N(T - T_0)]e^{-\frac{\Delta G^\circ}{RT}}}{1 + e^{-\frac{\Delta G^\circ}{RT}}}, \quad (1)$$

where S_N and S_D are the signal contributions from the native (N) and denatured (D) populations at $T_0 = 273.15$ K, m_N and m_D are the slope of the native and denatured state baselines and ΔG° is the free energy of folding. The free energy of folding is approximated as a linear function of temperature, $\Delta G^\circ \approx \delta g_1(T - T_m)$.³⁰ The data analysis was performed in IGOR PRO (WaveMetrics, Lake Oswego, OR).

Analysis of Kinetic Data. Relaxation kinetics of the proteins were collected and plotted as the ratio of the D/A intensity vs. time. The resulting transients were fit to a double exponential:³⁰

$$S(t) = S_0 + A_1 e^{-t/\tau_{laser}} + A_2 e^{-t/\tau_{obs}}, \quad (2)$$

where the first exponential accounts for the instrument response and relaxation of AcGFP1,²² and the second exponential accounts for the sample kinetics. S_0 is an offset, A_i are the amplitudes of the exponential decays, and τ are the relaxation lifetimes. We approximate both proteins here as two-state folders (single exponential folding relaxation kinetics).

RESULTS

Crowding Sensor CrH2-FRET Detects Changes in Crowder Concentration and Size. CrH2-FRET was expressed and purified to verify its ability to sense crowding.^{16,23,31} The sensor is comprised of CrH2 labeled by a green fluorescent protein (AcGFP1) donor (D) at the N-terminus and a mCherry acceptor (A) at the C-terminus (Figure 1A). The donor fluorescence-acceptor fluorescence ratio (D/A) reports on the end-to-end distance of the FRET construct. A large D/A (low FRET) is indicative of expansion, and, conversely, a small D/A (high FRET) is indicative of compaction.

To test the sensitivity of the sensor to crowding, the compaction of CrH2-FRET was measured in polyethylene glycol (PEG) *in vitro*. PEG, a straight-chain polymer of repeating units of ethylene glycol, is a common crowding agent.³² The effect of crowders on polymers can be described by the excluded-volume effect. The excluded-volume effect favors more compact conformations that occupy less volume due to the reduced conformational space available in a crowded solu-

tion.³³ Therefore, if CrH2-FRET is sensitive to crowding it should be compressed by increased crowding/excluded volume.

The sensitivity of CrH2-FRET to crowding was tested in two ways. First, crowding was increased by increasing the concentration of the crowder; CrH2-FRET was titrated with PEG 300 up to 25% (w/w = PEG mass / solvent mass) (Figure 1B, left). The excluded volume increased as there were more crowders in solution. Second, crowding was increased by increasing the size of the crowder; at a constant PEG concentration (10% w/w), the size of the PEG was increased up to 8 kD (Figure 1B, right). D/A was inversely correlated with both crowder size and crowder concentration, consistent with compaction of the sensor when crowder concentration or crowder size are increased (Figure 1B). These trends were also observed for a variant of CrH2-FRET labeled with mCitrine/mCerulean.¹⁶ Therefore, CrH2-FRET labeled with AcGFP1/mCherry behaves as expected and will be sensitive to crowding changes arising from both crowder concentration and crowder size in cells.

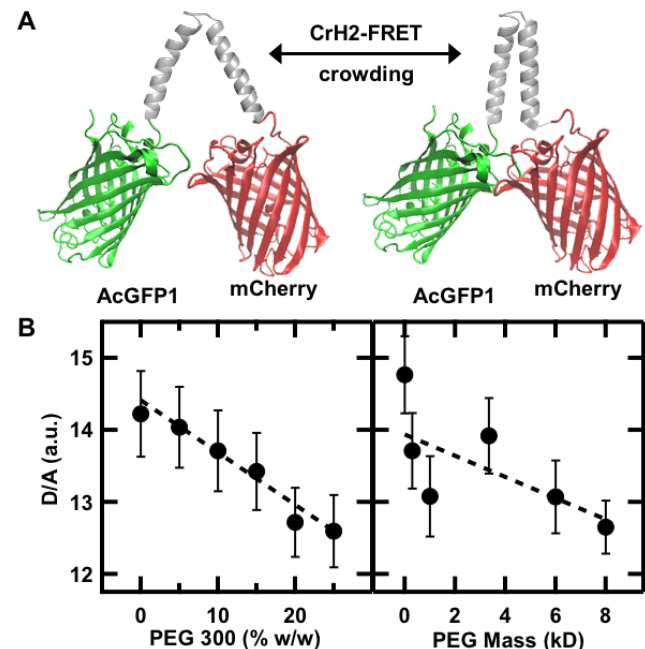


Figure 1. (A) Cartoon representation of CrH2-FRET illustrating conformational changes upon crowding. The doubly labeled FRET complex is labeled at the N-terminus with AcGFP1 and at the C-terminus with mCherry. AcGFP1 (PDB ID: 1GFL) and mCherry (PDB ID: 2H5Q) were generated in VMD³⁴ and the sensor was assembled in Adobe Photoshop CC. (B) CrH2-FRET donor/acceptor ratio versus PEG 300 concentration (left) and versus the molecular weight of PEG (10% w/w, right) at 21±1 °C. Error is the standard deviation of the mean of 3 measurements.

Compactness and Stability of PGK-FRET are Dependent on Crowder Concentration and Size *In Vitro*. PGK has been extensively used as a model protein for crowding studies because, similar to CrH2, its two subunits connected by a flexible hinge are sensitive to confinement (Figure 2A). PGK is a metabolic enzyme that undergoes a large-scale conformational change during catalysis in aqueous buffer.³⁵ Crowding not only compacts PGK, it increases its enzymatic activity and stabilizes its folding.³⁶ Past *in vitro* studies of the effect of

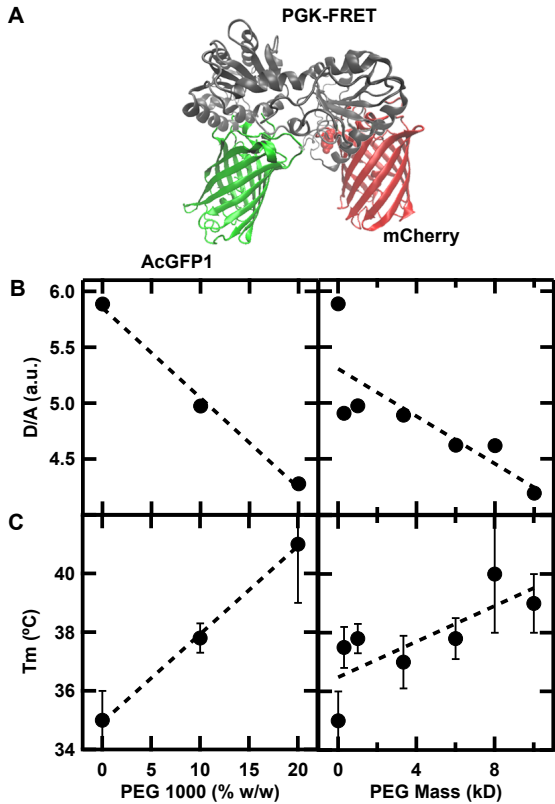


Figure 2. (A) Schematic representation of PGK-FRET labeled at the N-terminus with AcGFP1 and at the C-terminus with mCherry. Ribbon structures of PGK (PDB ID: 1QPG), GFP, and mCherry were generated in VMD³⁴ and assembled in Adobe Photoshop CC. The data for B and C are extracted from a representative experiment collected on a single day. (B) PGK-FRET donor/acceptor ratio versus PEG 1000 concentration (left) and versus the molecular weight of PEG (10% w/w, right) at 21±1 °C. Error bars are smaller than the data point. (C) PGK-FRET melting temperature versus PEG 1000 concentration (left) and versus the molecular weight of PEG (10% w/w, right). Melting temperatures (T_m) were extracted from a two-state model (Equation S1) fit of the thermal unfolding curves. Error is the standard deviation of the fit.

crowding on PGK increased crowding by increasing the concentration of crowder.^{17,23,36} The effect of crowder size on PGK compaction and stability has not been considered previously. Due to its sensitivity to crowder concentration and two-domain structure, we anticipate that the structure and stability of PGK-FRET are also sensitive to crowder size.

Indeed, increased excluded volume, induced by either crowder concentration or size, compacts and stabilizes PGK (Figure 2B,C). The same labeling strategy was used for PGK-FRET as for CrH2-FRET; PGK is labeled at the N-terminus by an AcGFP1 donor and C-terminus by a mCherry acceptor (Figure 2A). CrH2-FRET crowding experiments (Figure 1B) were replicated for PGK-FRET (Figure 2B). As was observed for CrH2-FRET, excluded volume was inversely correlated with the D/A of PGK-FRET; PGK-FRET is compacted by crowder concentration and size. Melting curves of PGK-FRET (Figure S1) were collected for each crowder condition and fit to an apparent two-state equilibrium model (Equation 1). Thermodynamic parameters derived from the fits are reported in Table S1-S2. Both fluorescent protein labels have melting points >70

°C, so changes in D/A with temperature report on conformational changes of PGK. The melting temperature of PGK is stabilized by increased excluded volume induced by crowder concentration or crowder size (Figure 2C). Therefore, both crowder concentration and crowder size may regulate the in-cell stability and compaction of PGK-FRET and likely other proteins.

PGK-FRET has already been shown to be sensitive to crowder concentration inside cells. *In vivo* comparison of PGK-FRET in differentiated tissues showed that folding was stabilized and slowed in the eye lens, the tissue with the highest amount of macromolecular crowding.³⁷ Individual cells experience different concentrations of crowders throughout their lifetime, for example in response to volume changes associated with mitosis. The unfolded state of PGK-FRET has been shown to be highly sensitive to crowding associated with cellular volume changes.^{38,39} While the sensitivity of PGK-FRET to crowder concentration in cells has been well characterized, the in-cell sensitivity of PGK-FRET to crowder size has yet to be tested.

Crowder Size and Crowder Concentration Changes Induced By Cytoskeletal Drugs Produce Competing Effects. Cells not only experience crowder concentration changes throughout their lifetime, the size of those crowders is also in flux. The cell's cytoskeleton is made of large dynamic protein assemblies, microtubules and actin filaments, that are constantly undergoing cycles of polymerization and depolymerization. For example, during cell migration actin filaments assemble at the leading edge and retract from the rear to help the cell move forward.⁴⁰ Microtubules quickly rearrange to form the mitotic spindle during cell division.⁴¹ These changes in turn affect cytoplasmic fluidity and the ability of other macromolecules in the cell to crowd.

To test the in-cell effect of cytoskeletal disassembly on protein structure and stability, we treated U-2 OS cells with cytoskeletal drugs that inhibit polymerization of actin (cytochalasin D, latrunculin B) or tubulin (nocodazole, vinblastine). Although all four drugs prevent polymerization they act by different mechanisms. Cytochalasin D caps the fast-growing end of microfilaments, preventing further polymerization.⁴² Latrunculin B inhibits new assembly by binding to actin monomers.⁴³ Nocodazole binds β -tubulin inducing curvature in the $\alpha\beta$ -tubulin heterodimer that hinders microtubule assembly.⁴⁴ Vinblastine binds at the interface between two $\alpha\beta$ -tubulin heterodimers obstructing tubulin self-association.⁴⁵ Inhibition of polymerization results in depolymerization and smaller crowder sizes because it shifts the monomer-polymer equilibrium towards dissociation.

U-2 OS cells were transfected with CrH2-FRET and incubated with the cytoskeletal drugs to determine the morphological changes associated with cytoskeletal perturbation. For each slide, four cells were imaged at the time the drug was added (SI XLSX file) and five cells were imaged following a ten-minute incubation (Figure 3 and SI XLSX file). Morphological changes typical of exposure to cytoskeletal drugs were observed, such as retraction from the substratum, apparent smaller size, and more “rounding” than untreated cells.^{46,47} To quantify the volume changes of our treated cells, we used 3D confocal microscopy to examine the volume of treated and untreated adhered U-2 OS cells (SI Cell Volume Measurements). We find that the cytoskeletal drugs we tested reduce the volume of treated U-2 OS cells by as much as 25% (Figure S2).

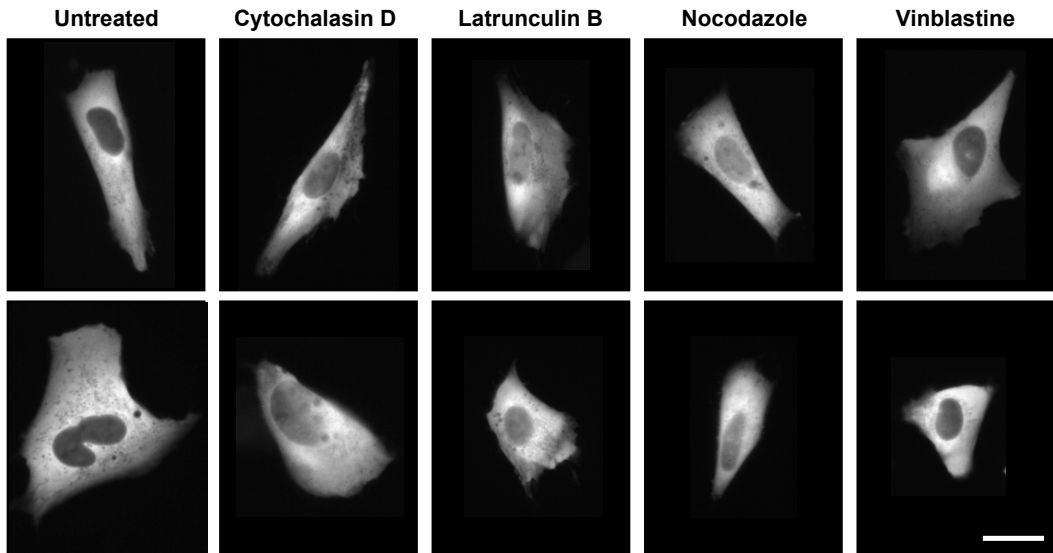


Figure 3. Representative effects of cytoskeletal drugs on cell morphology. Two representative cells treated by each cytoskeletal drug are presented here. U-2 OS cells were transfected with CrH2-FRET and cultured on glass coverslips at the time of transfection. Fluorescence images were collected following a 10-minute incubation with the cytoskeletal drug (see Experimental). The complete set of imaged cells transfected with CrH2-FRET, PGK-FRET, and VlsE-FRET are included in the SI XLSX file. PGK-FRET and VlsE-FRET were imaged between 10- and 30-minutes post incubation. All proteins are cytoplasmic. Scale bar is 30 μ m.

Our experiments suggest that the cell volume is not simply controlled by osmotic pressure. Considering the effect of osmotic pressure alone, depolymerization of the cytoskeleton increases the number of molecules in solution, increasing the osmotic pressure. Therefore, the cell volume should increase upon water intake to accommodate increased pressure. However, consistent with a past study,⁴⁸ we observe an inverse relationship between actin cytoskeleton structure and osmotic pressure. This supports a model^{49,50} where the cytoskeleton acts as an additional regulatory layer between the cell membrane and cytoplasm capable of resisting cell contraction (or expansion, depending on the state of the cell) as long as it remains assembled.

We consider the known effects of reduced cell volume, osmotic pressure, and hydrostatic pressure on protein structure and stability using macromolecular crowding theory.⁵¹ When cell volume decreases, the excluded volume increases and proteins are predicted to assume more compact and stable conformations. Osmotic pressure in the absence of cytoskeletal drugs also can be used to reduce cell volume, and CrH2-FRET compaction responds nearly linearly to osmotic volume reduction inside cells.³¹ Osmotic stress-induced volume changes of \pm 30% have temperature-dependent effects on the compaction of PGK-FRET.³⁹ Increased volumes had a negligible effect on protein stability and reduced volumes resulted in a ≤ 2 $^{\circ}$ C increase in PGK-FRET stability. Finally, we anticipate that the effect of hydrostatic pressure on protein compaction and folding is negligible under our conditions because the pressure necessary to unfold PGK-FRET is >600 bar.⁵² Therefore cytoskeletal drugs can produce two competing crowding effects inside cells: depolymerizing the cytoskeleton decreases crowder size and increases the fluidity of the cytoplasm, whereas reduced cell volume increases crowding.

Cytoskeletal Drugs Reduce Crowding In Cells. To determine how cytoskeletal drugs affect crowding in U-2 OS cells, the images of CrH2-FRET that were collected for morphologi-

cal studies (Figure 3) were also analyzed for change in D/A ratio. The change in D/A at 21 ± 1 $^{\circ}$ C following a 10-minute incubation with each cytoskeletal drug was measured (Figure 4). In all cases, addition of cytoskeletal drugs results in larger D/A values consistent with expansion of the CrH2-FRET sensor. We observed the same increase in D/A with decreasing crowder size *in vitro* (Figure 1B). Therefore we conclude that changes in crowding associated with cytoskeletal drugs are dominated by smaller crowder size and increased cytoplasmic fluidity upon cytoskeleton disassembly, not by reduced cell volume.

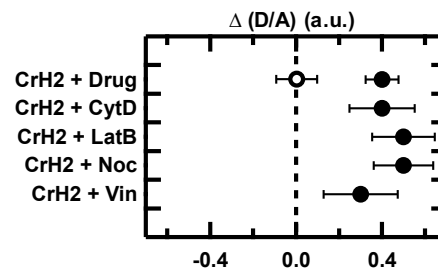


Figure 4. Change in donor/acceptor ratio at 21 ± 1 $^{\circ}$ C of CrH2-FRET in U-2 OS cells untreated (○) or treated (●) with cytoskeletal drugs: the average of all cytoskeletal drugs (Drug), cytochalasin D (CytD), latrunculin B (LatB), nocodazole (Noc), or vinblastine (Vin). Δ (D/A) is the difference in D/A between the reported condition and untreated CrH2-FRET. Error is the standard error of ≈ 50 measurements of treated or untreated cells or ≈ 15 measurements of each specific drug.

In Vitro Sensitivity to Crowding and Sticking Predicts In-Cell Protein Stability, Compactness, and Kinetics. Since cytoskeletal drugs decreased crowding inside cells, we predicted that protein stability, compactness, and kinetics would also be affected. The effect of cytoskeletal drugs on stability and compactness of two proteins with opposite sensitivities to

crowding were compared: crowding-sensitive PGK-FRET and

sticking-sensitive but crowding-insensitive VlsE-FRET. VlsE

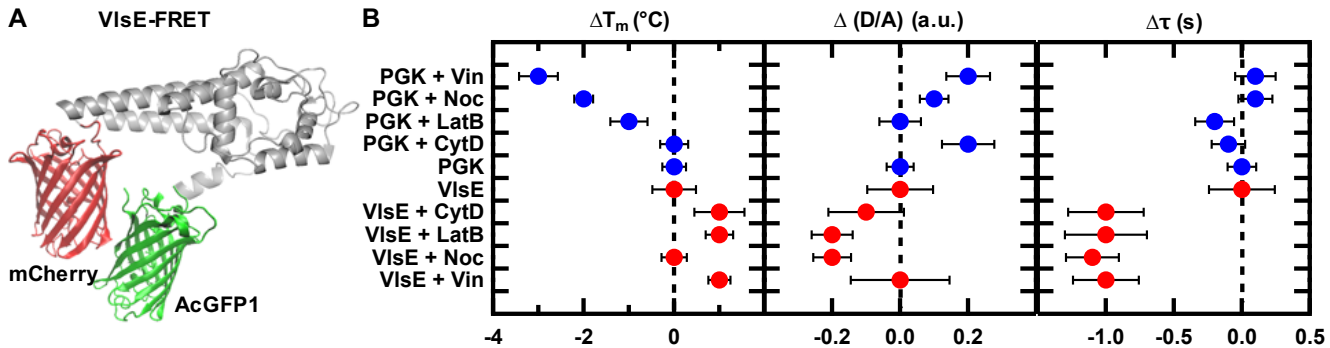


Figure 5. (A) Schematic representation of VlsE-FRET labeled at the N-terminus with AcGFP1 and at the C-terminus with mCherry. Ribbon structures of VlsE (PDB ID: 1L8W), GFP, and mCherry were generated in VMD³⁴ and assembled in Adobe Photoshop CC. (B) Change in thermal stability (left), change in donor/acceptor ratio (middle), and change in relaxation lifetime (right) of PGK (blue) and VlsE (red) in U-2 OS cells as a function of cytoskeletal drug. Cells were untreated or treated with Cytochalasin D (CytD), Latrunculin B (LatB), Nocodazole (Noc), or Vinblastine (Vin). (left) Melting temperatures (T_m) were extracted from a two-state model (Equation 1) fit of the thermal unfolding curves. ΔT_m is the difference in stability between the reported condition and untreated. (middle) $\Delta (D/A)$ is the difference in D/A between the reported condition and untreated cells at 21±1 °C. (right) Relaxation lifetimes were derived from a double exponential fit (Equation 2) of relaxation kinetics following a T-jump to the melting temperature. $\Delta \tau$ is the difference in relaxation lifetime between the reported condition and untreated. Error bars are the standard error of the reported condition, ≈15 VlsE measurements and ≈25 PGK measurements.

(Figure 5A) has a very different structure from PGK (Figure 2A) and CrH2 (Figure 1A). VlsE has a relatively rigid α -helical bundle structure, and this inflexibility causes a decreased sensitivity to crowding.¹⁷ Therefore, we hypothesized that decreased crowding arising from cytoskeletal drugs would destabilize and expand PGK-FRET and have little such effect on VlsE-FRET, but might slow down VlsE kinetics due to increased sticking. The same labeling strategy was used for VlsE-FRET (Figure 5A) as for PGK-FRET and CrH2-FRET; it is labeled at its N-terminus by AcGFP1 and its C-terminus by mCherry.

U-2 OS cells were transfected with PGK-FRET or VlsE-FRET and incubated with cytoskeletal drugs to determine the change in stability, compactness, and kinetics associated with decreased crowding induced by cytoskeletal drugs (Figure 5B). Melting curves (Figure S3) and transients (Figure S4) were collected for between five and nine cells per slide following a ten-minute incubation with the cytoskeleton drug. All thermal melts were collected between ten- and thirty-minutes post incubation. Melting curves were fit to an apparent two-state equilibrium model (Equation 1). Transients were fit to a double exponential where the first exponential accounts for the instrument response and relaxation of AcGFP1 in <200 ms, and the second exponential is the folding/unfolding relaxation kinetics of the protein (Equation 2). Thermodynamic and kinetic parameters derived from the fits are reported in Table S3-S4. As anticipated, decreased crowding resulting from the addition of cytoskeletal drugs noticeably destabilized PGK-FRET by up to 3 °C and had little effect on VlsE-FRET (stabilized by up to 1 °C) in Figure 5B, left.

Drugs that affected microtubules (vinblastine, nocodazole) were more destabilizing to PGK-FRET than drugs that affected actin filaments (cytochalasin D, latrunculin B). The role of the cytoskeleton is to organize the cell. Actin filaments are abundant beneath the cell membrane to assist with maintaining cell shape and architecture. Microtubules form a structural network through the cytoplasm and play a role in organization of cytoplasmic organelles. Depolymerization will loosen the

structure of the cell improving rotational and translational freedom. Since microtubules play a larger role in cytoplasmic organization,^{18,19} their depolymerization likely increases cell fluidity more than actin depolymerization.

Another possibility is that the larger monomer-polymer size differential of microtubules²⁰ leads to a larger change in excluded volume upon dissociation of microtubules than actin filaments. Although hard sphere crowding effects do not apply when the crowder is much larger than the protein being studied, microtubules and actin do not exist in a single population in cells; they dynamically populate a distribution of polymer lengths, including monomer such as G-actin.¹⁵ Treatment with cytoskeletal drugs pushes the polymer equilibria towards monomer. The size of actin and tubulin monomers are comparable: actin and tubulin are 42 and 55 kD, respectively. However, microtubules are significantly larger than actin filaments: in-cell, microtubules are ≈25 nm wide by as much as ≈1 mm long (in neurons)²⁰ and actin filaments are ≈6 nm wide by ≈10 μ m long⁵³. The increased width of microtubules decreases its flexibility, so the excluded volume of microtubules is greater than actin of the same length.⁵⁴ Therefore, depolymerization of microtubules results in a larger change in excluded volume and greater destabilization of PGK-FRET than depolymerization of actin.

The excluded volume effect predicts that decreased crowding destabilizes proteins, so reduced crowding alone in cells treated with cytoskeletal drugs cannot explain the slightly increased stability of VlsE-FRET. *In vitro*, VlsE-FRET is stabilized by inert macromolecular crowders as expected.¹⁷ However, the macromolecular crowders found inside cells are not inert. Non-specific surface interactions (sticking) between macromolecules inside cells can be stabilizing or destabilizing.⁵⁵ When microtubules and actin filaments depolymerize they increase the surface area available for sticking. Therefore, the change to the network of non-specific interactions caused by depolymerization may contribute to the slight stabilization of VlsE-FRET and destabilization of PGK-FRET.

Similarly a combination of crowding and non-specific interactions is necessary to explain the change in D/A of PGK-FRET and VlsE-FRET at 21 ± 1 °C (Figure 5B, middle). Addition of cytoskeletal drugs results in larger PGK-FRET D/A values consistent with expansion of the protein upon loss of crowding. In contrast, smaller VlsE-FRET D/A values are consistent with compaction, which cannot be explained by loss of crowding. In addition, the expansion and stability changes of PGK-FRET do not match the predicted *in vitro* values. For example, PGK-FRET + vinblastine in cells is destabilized by 3 °C and expanded by $\Delta(D/A) \approx 0.2$ (Figure 5B) but a similar 3 °C stability change *in vitro* corresponds to a $\Delta(D/A) \approx 0.8$ expansion (Figure 2B,C). *In vitro* experiments mimicking non-specific sticking in addition to crowding interactions can explain these observations: First, sticking in dilute cell lysate expands PGK-FRET and VlsE-FRET to a similar extent.¹⁷ Second, crowding compacts PGK-FRET more than VlsE-FRET.¹⁷ PGK-FRET is more sensitive to crowding so it is expanded by decreased crowding associated with cytoskeletal drugs and VlsE-FRET is more sensitive to sticking so it is compacted by new surface interactions with the depolymerized cytoskeletal filaments.

While most of the T_m and D/A data in Figure 5B are correlated, there are some inconsistencies in the observed trends (e.g. PGK + CytD). One possibility is that this deviation arises due to error in the measurement. Another possible explanation is that T_m and D/A are not fully correlated. For example, we have found that salt increases D/A of PGK and VlsE but has no effect on the T_m .¹⁷ Because all drugs act through different mechanisms, they may have different downstream effects.

The relaxation lifetimes of PGK-FRET and VlsE-FRET are also differently influenced by cytoskeletal drugs; PGK-FRET relaxation is unaffected and VlsE-FRET relaxation is sped up (Figure 5B, right). FReI was used to measure the relaxation kinetics near $\Delta G_u = 0$ ($k_f \approx k_u$) following a temperature jump to the protein's melting temperature of ~ 40 °C. The folding rate of PGK-FRET is insensitive to the *in vitro* and in-cell solvation environment,^{17,56} so it is unsurprising that environmental changes inside cells have no effect on the dynamics. On the other hand, there is a linear correlation between the stability and folding rate of VlsE-FRET measured in different solvation environments *in vitro*; increased protein stability is correlated with decreased relaxation lifetimes.¹⁷

The sensitivity of VlsE-FRET to the environment is increased three-fold inside cells compared to *in vitro*. We assess the relative environmental sensitivity by comparing the slope, $\Delta\text{Stability}$ (°C)/ $\Delta\text{Relaxation lifetime}$ (s), measured *in vitro* and in cells. To determine the slope *in vitro*, data from our previous studies of the VlsE-FRET¹⁷ were fit to a slope of -0.30 ± 0.2 (Figure S5). Inside cells the slope is ≈ -1 ; cytoskeletal drugs stabilized VlsE-FRET by ≈ 1 °C and its relaxation lifetime is sped by ≈ 1 s (Figure 5B).

DISCUSSION

Cellular structure is dynamic. Internal remodeling and exterior morphological changes are associated with many cellular processes, changing the intracellular environment that proteins interact with. The free energy landscape of proteins *in vivo* is sensitive to the local environment.^{30,38} While *in vitro* experiments can predict the responses of proteins to external perturbations,¹⁷ measurements in the cellular milieu are necessary to fully characterize protein folding landscapes, which depend on

the solvation environment. Recently, an *in vitro* investigation demonstrated that crowder size has an asymmetrical effect on the heat and cold-denatured folding, with cold-denatured states being more expanded.⁵⁷ To determine how structural remodeling impacts protein stability and folding kinetics inside cells, we treated living U-2 OS cells with cytoskeletal drugs that depolymerize large structural units in the cell, microtubules and actin filaments. Our hypothesis is that cytoskeleton disassembly leads to smaller crowders and decreases crowding either directly, or indirectly by increasing the fluidity of the cytoplasmic matrix.

While our crowding sensor and crowding-sensitive protein PGK-FRET exhibit characteristics consistent with decreased crowding, the crowding-insensitive protein VlsE-FRET responds to depolymerization in ways that cannot be accounted for by crowding alone. The concept of steric crowding says that reactions that increase the translational and rotational freedom (e.g. compaction, folding, association) will be favored in a crowded environment.⁵⁸ While steric crowding interactions can accurately model inert crowders,^{59,60} they fail to account for non-steric surface interactions,¹³ such as in the sticky cellular milieu. VlsE-FRET's atypical slight stabilization and contraction in response to decreased crowding suggests that depolymerization of the cytoskeleton affects the network of non-steric interactions in the cell. The sensitivity of VlsE-FRET to reduced crowding was increased over *in vitro* predictions,¹⁷ so the exact mechanism behind these changes, whether direct interaction of VlsE with monomers such as G-actin, or indirect effects due to changes in the cytoplasmic matrix after depolymerization, remains to be investigated.

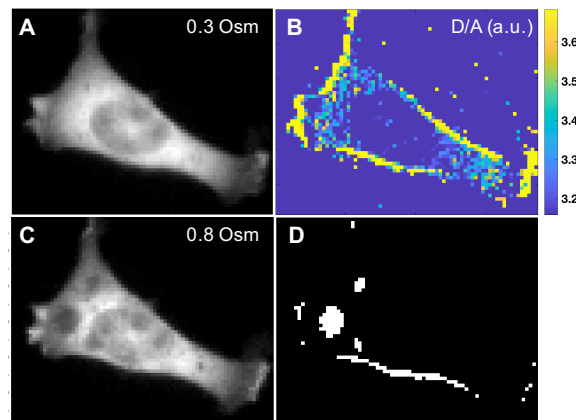


Figure 6. Representative U-2 OS cell transfected with low melting temperature PGK-FRET and imaged under (A) isosmotic and (C) hyperosmotic conditions. (B) The D/A of the isosmotic cell (A) imaged at 33 °C. Each pixel is color-coded on a scale from smaller D/A ratios (dark blue) to larger D/A ratios (yellow to light blue). PGK is less compact in the yellow and light blue regions. (D) Areas of reduced cytoskeletal density as mapped by osmotic stress (comparing the cells in (A) and (C)). The areas of lower cytoskeletal density in (D) correlate with the areas of less compact PGK in (B).

Our results suggest that the cytoskeleton modulates the intracellular conformational distribution of proteins. In particular, we predict that proteins are less compact in the absence of local cytoskeleton structure. To test this prediction, we compared the D/A of PGK-FRET localized in regions where cyto-

skeleton is sparse to other regions of the cell. We re-analyzed 60 U-2 OS cells expressing a low-melting variant of PGK-FRET³⁹ (Figure 6A, Table S5, SI section ‘Re-Analysis of Osmotic Data’) to determine D/A near the protein’s melting point (Figure 6B; orange to light blue = larger D/A ratios, dark blue = smaller D/A ratios). We then used osmotic stress (Figure 6C) to identify regions where the membrane has fewer cytoskeletal attachments (Figure 6D): the cytoskeletal network is coupled to the cell membrane,⁶¹ and under stress deformations occur in positions where the membrane is unsupported.⁶² Regions of high D/A in Figure 6B are correlated with regions where the membrane has fewer cytoskeletal attachments. Thus, we find that PGK-FRET in the regions least populated by cytoskeleton is less compact than PGK-FRET localized in regions with more cytoskeleton. This observation demonstrates that cytoskeletal structure can locally regulate protein structure and stability.

Although the effect of crowder concentration has been considered inside cells,^{38,39} this is the first evidence that crowder size *via* disassembly can also modulate protein energy landscapes in-cell. Our results suggest that local remodeling of the cell, for example during cell migration or mitosis, results in local differences in the stability of proteins. Vinblastine, the cytoskeletal drug that had the largest effect on PGK-FRET, is an approved drug used for chemotherapy. Although limited in their effectiveness, such natural compounds that target microtubules are among the best chemotherapeutic drugs available.⁶³ One possible reason for adverse side effects associated with microtubule-targeting drugs is that their delivery is often untargeted, so cytoplasmic macromolecules beyond those in targeted cells will be affected.

CONCLUSION

Our results raise the possibility that regulation of the protein energy landscape is locally controlled by cytoskeleton dynamics: during cell migration the same protein located near actin filaments assembled at the leading edge may have a different stability and compactness from proteins near the rear where actin filaments disassemble. In fact, one might expect a gradient of environments across the cell. This has important implications for proteins with transient elements, protein-protein interactions involved in protein signaling, disordered proteins, or storage in liquid droplets. Since cellular structural elements are constantly in flux, these types of proteins may be more conformationally dynamic than predicted by measurements under a single crowding concentration.

ASSOCIATED CONTENT

SI

The SI is available free of charge on the ACS Publications website.

Plots of representative *in vitro* temperature denaturation of PGK-FRET, melt curves of PGK-FRET and VlsE-FRET collected in living U-2 OS cells, transients of PGK-FRET and VlsE-FRET, relaxation lifetime measured at T_m vs. melting temperature of VlsE-FRET and complete tables of thermodynamic and kinetic parameters obtained *in vitro* and in living U-2 OS cells. (PDF file)

Fluorescence images of all cells analyzed. (XLSX file)

Accession Codes

B. burgdorferi VlsE sequence, UniProtKB 006878; *S. cerevisiae* PGK sequence, UniProtKB P00560.

AUTHOR INFORMATION

Corresponding Authors

* c.davis@yale.edu, mgruebel@illinois.edu

Present Addresses

† Department of Chemistry, Yale University, 225 Prospect St., New Haven, CT, 06520 USA

Author Contributions

The manuscript was written through contributions of all authors. All authors have given approval to the final version of the manuscript.

ACKNOWLEDGMENT

This work was supported by the National Institutes of Health grant R01GM093318 (*in vitro* work) and National Science Foundation (NSF) grant NSF MCB 1803786 (in-cell work) to M.G. C.M.D. was supported in part by a postdoctoral fellowship provided by the PFC: Center for the Physics of Living Cells funded by NSF PHY 1430124. We thank Shahar Sukenik for performing imaging and volumetric analysis of 3D confocal images.

REFERENCES

- (1) Zimmerman, S. B.; Trach, S. O. Estimation of Macromolecule Concentrations and Excluded Volume Effects for the Cytoplasm of *Escherichia Coli*. *J. Mol. Biol.* **1991**, *222*, 599–620.
- (2) Minton, A. P. The Influence of Macromolecular Crowding and Macromolecular Confinement on Biochemical Reactions in Physiological Media. *J. Biol. Chem.* **2001**, *276*, 10577–10580.
- (3) Lee, S. H.; Dominguez, R. Regulation of Actin Cytoskeleton Dynamics in Cells. *Mol. Cells* **2010**, *29*, 311–325.
- (4) Brouhard, G. J.; Rice, L. M. Microtubule Dynamics: An Interplay of Biochemistry and Mechanics. *Nat. Rev. Mol. Cell Biol.* **2018**, *19*, 451–463.
- (5) Meunier, S.; Vernos, I. Microtubule Assembly during Mitosis – from Distinct Origins to Distinct Functions? *J. Cell Sci.* **2012**, *125*, 2805–2814.
- (6) Hussey, P. J.; Ketelaar, T.; Deeks, M. J. CONTROL OF THE ACTIN CYTOSKELETON IN PLANT CELL GROWTH. *Annu. Rev. Plant Biol.* **2006**, *57*, 109–125.
- (7) McMahon, H. T.; Gallop, J. L. Membrane Curvature and Mechanisms of Dynamic Cell Membrane Remodelling. *Nature* **2005**, *438*, 590–596.
- (8) Burkhardt, J. K. Cytoskeletal Function in the Immune System. *Immunol. Rev.* **2013**, *256*, 5–9.
- (9) Lamacice, L.; Le Boeuf, F.; Huot, J. Endothelial Cell Migration During Angiogenesis. *Circ. Res.* **2007**, *100*, 782–794.
- (10) Hinz, B. Formation and Function of the Myofibroblast during Tissue Repair. *J. Invest. Dermatol.* **2007**, *127*, 526–537.
- (11) Mu, X.; Choi, S.; Lang, L.; Mowray, D.; Dokholyan, N. V.; Danielsson, J.; Oliveberg, M. Physicochemical Code for Quininary Protein Interactions in *Escherichia Coli*. *Proc. Natl. Acad. Sci.* **2017**, *114*, E4556–E4563.
- (12) Sarkar, M.; Li, C.; Pielak, G. J. Soft Interactions and Crowding. *Biophysical Reviews*. 2013, pp 187–194.
- (13) Muramatsu, N.; Minton, A. P. Hidden Self-Association of Proteins. *J. Mol. Recognit.* **1989**, *1*, 166–171.
- (14) Belmont, L. D.; Mitchison, T. J. Identification of a Protein That Interacts with Tubulin Dimers and Increases the Catastrophe Rate of Microtubules. *Cell* **1996**, *84*, 623–631.
- (15) Ünlü, A. Computational Prediction of Actin–Actin Interaction. *Mol. Biol. Rep.* **2014**, *41*, 355–364.
- (16) Boersma, A. J.; Zuhorn, I. S.; Poolman, B. A Sensor for Quantification of Macromolecular Crowding in Living Cells. *Nat. Methods* **2015**, *12*, 227–229.
- (17) Davis, C. M.; Gruebele, M. Non-steric Interactions Predict the

- (18) Trend and Steric Interactions the Offset of Protein Stability in Cells. *ChemPhysChem* **2018**, *19*, 2290–2294.
- (19) Cole, N. B.; Lippincott-Schwartz, J. Organization of Organelles and Membrane Traffic by Microtubules. *Curr. Opin. Cell Biol.* **1995**.
- (20) Fritzsche, M.; Li, D.; Colin-York, H.; Chang, V. T.; Moeendarbary, E.; Felce, J. H.; Sezgin, E.; Charras, G.; Betzig, E.; Eggeling, C. Self-Organizing Actin Patterns Shape Membrane Architecture but Not Cell Mechanics. *Nat. Commun.* **2017**, *8*, 14347.
- (21) Wen, Q.; Janmey, P. A. Polymer Physics of the Cytoskeleton. *Curr. Opin. Solid State Mater. Sci.* **2011**, *15*, 177–182.
- (22) Ebbinghaus, S.; Dhar, A.; McDonald, J. D.; Gruebele, M. Protein Folding Stability and Dynamics Imaged in a Living Cell. *Nat. Methods* **2010**, *7*, 319–323.
- (23) Guzman, I.; Gelman, H.; Tai, J.; Gruebele, M. The Extracellular Protein VlsE Is Destabilized inside Cells. *J. Mol. Biol.* **2014**, *426*, 11–20.
- (24) Kisley, L.; Serrano, K. A.; Guin, D.; Kong, X.; Gruebele, M.; Leckband, D. E. Direct Imaging of Protein Stability and Folding Kinetics in Hydrogels. *ACS Appl. Mater. Interfaces* **2017**, *9*, 21606–21617.
- (25) Wakatsuki, T.; Schwab, B.; Thompson, N. C.; Elson, E. L. Effects of Cytochalasin D and Latrunculin B on Mechanical Properties of Cells. *J. Cell Sci.* **2001**, *114*, 1025–1036.
- (26) Oka, T.; Hori, M.; Ozaki, H. Microtubule Disruption Suppresses Allergic Response through the Inhibition of Calcium Influx in the Mast Cell Degranulation Pathway. *J. Immunol.* **2014**, *174*, 4584–4589.
- (27) Salerni, B. L.; Bates, D. J.; Albershardt, T. C.; Lowrey, C. H.; Eastman, A. Vinblastine Induces Acute, Cell Cycle Phase-Independent Apoptosis in Some Leukemias and Lymphomas and Can Induce Acute Apoptosis in Others When Mcl-1 Is Suppressed. *Mol. Cancer Ther.* **2010**, *9*, 791–802.
- (28) Kretz, R.; Wendt, L.; Wongkanoun, S.; Luangsa-ard, J.; Surup, F.; Helaly, S.; Noumeur, S.; Stadler, M.; Stradal, T. The Effect of Cytochalasans on the Actin Cytoskeleton of Eukaryotic Cells and Preliminary Structure–Activity Relationships. *Biomolecules* **2019**, *9*, 73.
- (29) Couch, R. D.; Ganem, N. J.; Zhou, M.; Popov, V. M.; Honda, T.; Veenstra, T. D.; Sporn, M. B.; Anderson, A. C. 2-Cyano-3,12-Dioxoleane-1,9(11)-Diene-28-Oic Acid Disrupts Microtubule Polymerization: A Possible Mechanism Contributing to Apoptosis. *Mol. Pharmacol.* **2006**, *69*, 1158–1165.
- (30) Wang, X.; Tanaka, M.; Krstin, S.; Peixoto, H. S.; Wink, M. The Interference of Selected Cytotoxic Alkaloids with the Cytoskeleton: An Insight into Their Modes of Action. *Molecules* **2016**.
- (31) Dhar, A.; Girdhar, K.; Singh, D.; Gelman, H.; Ebbinghaus, S.; Gruebele, M. Protein Stability and Folding Kinetics in the Nucleus and Endoplasmic Reticulum of Eucaryotic Cells. *Biophys. J.* **2011**, *101*, 421–430.
- (32) Sukenik, S.; Ren, P.; Gruebele, M. Weak Protein–Protein Interactions in Live Cells Are Quantified by Cell-Volume Modulation. *Proc. Natl. Acad. Sci. U. S. A.* **2017**, *114*, 6776–6781.
- (33) Phillip, Y.; Sherman, E.; Haran, G.; Schreiber, G. Common Crowding Agents Have Only a Small Effect on Protein–Protein Interactions. *Biophys. J.* **2009**, *97*, 875–885.
- (34) Minton, A. P. Excluded Volume as a Determinant of Protein Structure and Stability. *Biophys. J.* **1980**, *32*, 77–79.
- (35) Humphrey, W.; Dalke, A.; Schulten, K. VMD: Visual Molecular Dynamics. *J. Mol. Graph.* **1996**, *14*, 33–38.
- (36) Gerstein, M.; Lesk, A. M.; Chothia, C. Structural Mechanisms for Domain Movements in Proteins. *Biochemistry* **1994**, *33*, 6739–6749.
- (37) Dhar, A.; Samiotakis, A.; Ebbinghaus, S.; Nienhaus, L.; Homouz, D.; Gruebele, M.; Cheung, M. S. Structure, Function, and Folding of Phosphoglycerate Kinase Are Strongly Perturbed by Macromolecular Crowding. *Proc. Natl. Acad. Sci.* **2010**, *107*, 17586–17591.
- (38) Feng, R.; Gruebele, M.; Davis, C. M. Quantifying Protein Dynamics and Stability in a Living Organism. *Nat. Commun.* **2019**, *10*, e1179.
- (39) Wirth, A. J.; Platkov, M.; Gruebele, M. Temporal Variation of a Protein Folding Energy Landscape in the Cell. *J. Am. Chem. Soc.* **2013**, *135*, 19215–19221.
- (40) Wang, Y.; Sukenik, S.; Davis, C. M.; Gruebele, M. Cell Volume Controls Protein Stability and Compactness of the Unfolded State. *J. Phys. Chem. B* **2018**, *122*, 11762–11770.
- (41) Spooner, B. S.; Yamada, K. M.; Wessells, N. K. MICROFILAMENTS AND CELL LOCOMOTION. *J. Cell Biol.* **1971**, *49*, 595–613.
- (42) Gadde, S.; Heald, R. Mechanisms and Molecules of the Mitotic Spindle. *Curr. Biol.* **2004**, *14*, R797–R805.
- (43) Cooper, J. A. Effects of Cytochalasin and Phalloidin on Actin. *J. Cell Biol.* **1987**, *105*, 1473–1478.
- (44) Spector, I.; Shochet, N.; Kashman, Y.; Graweiss, A. Latrunculins: Novel Marine Toxins That Disrupt Microfilament Organization in Cultured Cells. *Science (80-.)* **1983**, *219*, 493–495.
- (45) Ravelli, R. B. G.; Gigant, B.; Curmi, P. A.; Jourdain, I.; Lachkar, S.; Sobel, A.; Knossow, M. Insight into Tubulin Regulation from a Complex with Colchicine and a Stathmin-like Domain. *Nature* **2004**, *428*, 198–202.
- (46) Gigant, B.; Wang, C.; Ravelli, R. B. G.; Roussi, F.; Steinmetz, M. O.; Curmi, P. A.; Sobel, A.; Knossow, M. Structural Basis for the Regulation of Tubulin by Vinblastine. *Nature* **2005**, *435*, 519–522.
- (47) Clark, A. G.; Paluch, E. Mechanics and Regulation of Cell Shape During the Cell Cycle. In *Results and Problems in Cell Differentiation*; 2011; pp 31–73.
- (48) Stewart, M. P.; Helenius, J.; Toyoda, Y.; Ramanathan, S. P.; Muller, D. J.; Hyman, A. A. Hydrostatic Pressure and the Actomyosin Cortex Drive Mitotic Cell Rounding. *Nature* **2011**, *469*, 226–230.
- (49) Stewart, M. P.; Helenius, J.; Toyoda, Y.; Ramanathan, S. P.; Muller, D. J.; Hyman, A. A. Hydrostatic Pressure and the Actomyosin Cortex Drive Mitotic Cell Rounding. *Nature* **2011**, *469*, 226–230.
- (50) Keren, K.; Yam, P. T.; Kinkhabwala, A.; Mogilner, A.; Theriot, J. A. Intracellular Fluid Flow in Rapidly Moving Cells. *Nat. Cell Biol.* **2009**, *11*, 1219–1224.
- (51) Mitchison, T. J.; Charras, G. T.; Mahadevan, L. Implications of a Poroelastic Cytoplasm for the Dynamics of Animal Cell Shape. *Semin. Cell Dev. Biol.* **2008**, *19*, 215–223.
- (52) Minton, A. P. How Can Biochemical Reactions within Cells Differ from Those in Test Tubes? *J. Cell Sci.* **2006**, *119*, 2863–2869.
- (53) Chen, T.; Dave, K.; Gruebele, M. Pressure- and Heat-induced Protein Unfolding in Bacterial Cells: Crowding vs. Sticking. *FEBS Lett.* **2018**, *592*, 1357–1365.
- (54) Ott, A.; Magnasco, M.; Simon, A.; Libchaber, A. Measurement of the Persistence Length of Polymerized Actin Using Fluorescence Microscopy. *Phys. Rev. E* **1993**, *48*, R1642–R1645.
- (55) McGrath, J. L. Microtubule Mechanics: A Little Flexibility Goes a Long Way. *Curr. Biol.* **2006**, *16*, R800–R802.
- (56) McConkey, E. H. Molecular Evolution, Intracellular Organization, and the Quininary Structure of Proteins. *Proc. Natl. Acad. Sci.* **1982**, *79*, 3236–3240.
- (57) Gelman, H.; Wirth, A. J.; Gruebele, M. ReASH as a Quantitative Probe of In-Cell Protein Dynamics. *Biochemistry* **2016**, *55*, 1968–1976.
- (58) Alfano, C.; Sanfelice, D.; Martin, S. R.; Pastore, A.; Temussi, P. A. An Optimized Strategy to Measure Protein Stability Highlights Differences between Cold and Hot Unfolded States. *Nat. Commun.* **2017**, *8*, 15428.
- (59) Zhou, H.-X.; Rivas, G.; Minton, A. P. Macromolecular Crowding and Confinement: Biochemical, Biophysical, and Potential Physiological Consequences. *Annu. Rev. Biophys.* **2008**, *37*, 375–397.
- (60) Hall, D.; Minton, A. P. Macromolecular Crowding: Qualitative and Semiquantitative Successes, Quantitative Challenges. *Biochim. Biophys. Acta - Proteins Proteomics* **2003**, *1649*, 127–139.
- (61) Gnutt, D.; Gao, M.; Brylski, O.; Heyden, M.; Ebbinghaus, S. Excluded-Volume Effects in Living Cells. *Angew. Chemie - Int. Ed.* **2015**, *54*, 2548–2551.

- (61) Le Roux, A.-L.; Quiroga, X.; Walani, N.; Arroyo, M.; Roca-Cusachs, P. The Plasma Membrane as a Mechanochemical Transducer. *Philos. Trans. R. Soc. B Biol. Sci.* **2019**, *374*, 20180221.
- (62) Pocivavsek, L.; Dellsy, R.; Kern, A.; Johnson, S.; Lin, B.; Lee, K. Y. C.; Cerdá, E. Stress and Fold Localization in Thin Elastic Membranes. *Science (80-.)* **2008**, *320*, 912–916.
- (63) Mukhtar, E.; Adhami, V. M.; Mukhtar, H. Targeting Microtubules by Natural Agents for Cancer Therapy. *Mol. Cancer Ther.* **2014**, *13*, 275–284.

Authors are required to submit a graphic entry for the Table of Contents (TOC) that, in conjunction with the manuscript title, should give the reader a representative idea of one of the following: A key structure, reaction, equation, concept, or theorem, etc., that is discussed in the manuscript. Consult the journal's Instructions for Authors for TOC graphic specifications.

